

Yields of K and L X Rays Arising from 2–30-MeV-Proton Bombardment of Ag^\dagger

G. A. Bissinger* and S. M. Shafroth

University of North Carolina, Chapel Hill, North Carolina 27514
and Triangle Universities Nuclear Laboratory, Durham, North Carolina 27706

and

A. W. Waltner

North Carolina State University, Raleigh, North Carolina 27607
and Triangle Universities Nuclear Laboratory, Durham, North Carolina 27706

(Received 26 July 1971)

Ag K and L x-ray yields have been measured for 2–30-MeV protons incident on a thin Ag foil target with a Si(Li) x-ray detector (resolution 540 eV at 6 keV). The absolute K -shell ionization cross section σ_K extracted from these measurements has been compared to plane-wave-Born-approximation (PWBA) and binary-encounter-approximation (BEA) calculations and agrees quite well with both over the energy range covered in this investigation. However, the PWBA and BEA predictions of L -shell ionization cross sections are low by a factor close to 2 compared to experimental values for σ_L , although both predict an energy dependence for the shape of σ_L in good agreement with that observed. The disagreement in magnitude is most likely because of the present inadequate L -shell fluorescence yields for medium- and low- Z atoms. The $K\alpha/K\beta$ x-ray intensity ratio for proton bombardment of Ag from 2–30 MeV was observed to be constant (4.68 ± 0.33) and consistently slightly below Scofield's calculation (5.09). The unresolved $K\beta$ peak was decomposed into its two major components $K\beta_{1,3}$ and $K\beta_2$ whose ratio appeared to be weakly dependent on proton-beam energy.

I. INTRODUCTION

There is now a large amount of reliable information available on proton-induced K -shell ionization cross sections for proton energies below 4 MeV,^{1–4} over nearly the entire Periodic Table. However, measurements with proton beams of energies greater than 4 MeV are still scarce. At present there exist measurements for higher-energy protons only on Ca, Ti, Ni,⁵ and Cu.⁶ This work extends these measurements to Ag ($Z = 47$) and presents measurements of K - and L -shell ionization cross sections for proton energies from 2–30 MeV.

The present theories of inner-shell ionization processes have been quite successful in the case of proton projectiles. The plane-wave-Born-approximation (PWBA) predictions^{1,7} for K -shell ionization cross sections, which do not correct for nuclear repulsion, electron orbit polarization, or relativistic effects, agree well with experimental measurements near the predicted maximum in cross section (when the ionizing projectile's velocity equals the mean velocity of the K electrons) but tend to fall above the experimental values for lower proton energies. Improved agreement for lower proton energies is obtained in the approach of Bang and Hansteen,⁸ who provide for the effects of nuclear repulsion by describing the incident particle by its classical hyperbolic trajectory (a straight-line trajectory gives the PWBA results).

However, this method requires more partial waves in the final-state electron continuum as the beam energy is increased, and so the available calculations are best for the lower beam energies. The most recent approach to the problem of K -shell ionization by protons is that of Garcia,² who uses the binary-encounter (impulse) approximation (BEA) (where a direct energy exchange between the proton and the inner-shell electron through the Coulomb interaction is assumed) to examine inner-shell ionization, including the effects of nuclear repulsion on the proton. The BEA predictions are quite close to those of Bang and Hansteen for lower-energy protons, while for higher-energy protons they tend to be quite close to PWBA results. However, for higher Z the PWBA and BEA predictions tend to agree somewhat better at lower energies also, because the screening corrections in the PWBA theory tend to displace the maximum of the cross section toward higher proton energies. The BEA model is very simple and permits direct scaling of cross sections for all Z from calculated cross sections for $Z = 12$ according to the binding energy of the K -shell electron.

Recent experiments by Basbas *et al.*⁹ and by Lewis *et al.*¹⁰ tested the z^2 (projectile z) dependence of σ_K predicted by PWBA (this same dependence is also predicted by BEA if the differences in nuclear repulsion are neglected) using proton and α -particle beams and deuteron and α -particle beams,

respectively. Taking the ratio of cross sections at the same velocity permits many experimental and theoretical simplifications and is more reliable and exacting than comparison of experimental and theoretical results for $\sigma_K(p)$, $\sigma_K(d)$, or $\sigma_K(\alpha)$ alone. These experiments revealed an energy dependence in the experimental ratio of cross sections in contrast to the theoretical prediction of a constant ratio. This energy dependence could not be predicted by PWBA even when the Coulomb deflection and binding-energy corrections to PWBA proposed by Brandt, Laubert, and Sellin¹¹ were applied. Considerably larger discrepancies from PWBA calculated cross sections are observed for heavy-ion projectiles.¹²⁻¹⁴

The present work also reports Ag L-shell ionization cross sections for protons from 2-30 MeV and compares these experimental results with PWBA and BEA predictions.

$K\alpha/K\beta$ x-ray intensity ratios for Ag were studied as a function of proton energy and compared with other work as well as with recent theoretical calculations^{15,16} of these ratios. An attempt was made to study $K\beta_{1,3}/K\beta_2$ intensity ratios as a function of proton-beam energy. A preliminary account of some of this work has been given.¹⁷

II. EXPERIMENTAL

A. Apparatus

Proton beams from 17 to 30 MeV were obtained from the Triangle Universities Nuclear Laboratory Cyclo-Graaff¹⁸ facility, which consists of a fixed-energy ($E_p = 15$ MeV) negative-ion AVF (alternating valley focusing) cyclotron injecting into a model FN tandem Van de Graaff, while 2-15 MeV beams were provided by the tandem alone. These beams were used to bombard thin self-supporting foil targets of Ag suspended in a target chamber with a thin Mylar-foil window 1 in. in diameter, 1.625

in. from the center of the chamber. Beam current was integrated in a 2-in.-diam 8-ft-long aluminum pipe insulated from the target chamber by two delrin sections which sandwiched an isolated length of beam pipe 6 in. long which in turn was connected to a 600-V battery for electron suppression. The beam dump was located 9 ft from the chamber behind ~3 ft of paraffin and concrete-block shielding. No degradation of spectra for proton energies near 30 MeV was observed. The beam was focused on a beam stop 4 ft in front of the chamber and then passed through an insulated collimator $\frac{1}{8}$ in. in diameter, 1 ft upstream of the target. Beam focus was then adjusted for minimum beam on this collimator. In practice, it was not difficult to pass 98% of the beam through this collimator. Since the last focusing quadrupole on this beam leg was 30-ft upstream of the target, a $\frac{1}{8}$ -in.-diam beam spot on the target was ensured.

The x-ray detector used in this experiment was a liquid-nitrogen-cooled Si(Li) detector of 22.8-mm² area with a resolution of ~540 eV for the Cu $K\alpha$ line and ~630 eV for the Ag $K\alpha$ line. The detector was placed at a 90° angle to the beam, 8.74 cm from the target with an air path of 4.60 cm from the Mylar window. A typical x-ray spectrum collected for 13-MeV protons on Ag is shown in Fig. 1. The air and Mylar-window absorption were corrected for in these measurements. These corrections were significant only for the Ag L x rays (~3.2 KeV). A description of the experimental arrangement [excepting the Si(Li) detector and its associated electronics] has been given earlier.⁵

B. Efficiency Calibration

The efficiency of the Si(Li) detector was determined in the following manner. The intrinsic efficiency of this detector was assumed to be 1.0 at $E_\gamma = 14$ keV, since more than 99.9% of the incident

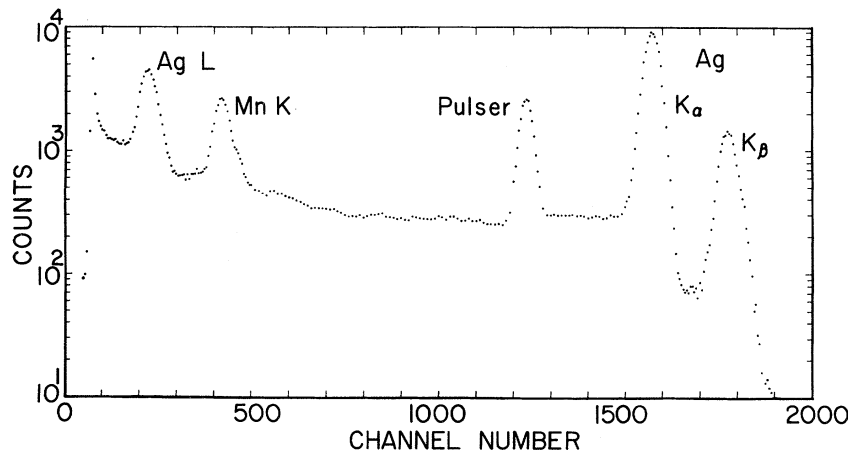


FIG. 1. Pulse-height spectrum arising from 13-MeV-proton bombardment of Ag. Also shown is an unresolved K x-ray peak at about 5.9 keV due to a ⁵⁵Fe calibration source, as well as a pulser peak for deadtime correction and secondary energy calibration.

photons would be absorbed in 3 mm of silicon. From 14–26 keV the relative efficiency calibration was performed using a thin ^{241}Am source which provided ^{237}Np L x rays from 13–17 keV as well as a 26-keV γ ray.¹⁹

The low-energy portion of the efficiency curve was determined by comparing the relative intensity of the Fe K x rays (6.40 keV) and the 14.38-keV γ ray of ^{57}Fe as seen by the Si(Li) detector and a Xe-filled proportional counter having the same Be window thickness (0.010 in.). A relatively higher x-ray intensity was observed in the Xe counter presumably owing to dead layers of Si and Au present in the Si(Li) detector. For energies less than 6.40 keV, a relative efficiency curve based on the Mn K x-ray and the Ag L x-ray intensities from a composite ^{109}Cd – ^{55}Fe source was obtained. As there was no overlap of the two low-energy relative efficiency curves between 6.40 and 5.90 keV, the curves were combined in this region by means of an empirical Fe/Mn efficiency ratio which was calculated assuming continuity for the detector-efficiency curve. The resulting efficiency curve was then corrected for the x-ray absorption of the 0.010-in. Be window and joined to the intrinsic efficiency curve at 14.0 keV. It was found that relative to the efficiency at 14.38 keV, the Si(Li) detector efficiency for the Ag L x rays (3.4 keV) was 0.098 ± 0.010 , while that for the Fe x ray (6.4 keV) was 0.40 ± 0.02 .

For the determination of the absolute intrinsic efficiency, the solid angle subtended by the detector at the source distance for the experiment was determined by comparing the counting rate for the 14.38-keV ^{57}Co γ ray with and without a well-centered Al mask which had an accurately known aperture. The solid angle thus obtained was 2.05×10^{-4} sr at 8.74 cm.

C. Targets

The Ag target consisted of a thin, self-supporting foil whose thickness was measured by Rutherford scattering of 6.00-MeV α particles at 30° (lab). In addition, the uniformity of this target was checked by moving the target transverse to the beam and determining the thickness at three points, as well as rotating the target at various angles to the beam. The Ag target thickness was measured as $30.9 \pm 3.5 \times 10^{-6}$ cm.

D. Analysis and Calibrations

The peaks in the x-ray spectra were fit with a Gauss-fit program which was capable of fitting up to two Gaussians and a quadratic background simultaneously. The Gauss-fit program was used to determine x-ray line intensities, while centroid calculations, after linear background subtraction, were used to determine possible energy shifts of

the x-ray lines.

E. Energy Calibrations and Dead Time Corrections

Energy calibrations for the Ag spectra were provided by a 5.90-keV x ray of ^{55}Fe and a precision pulser. The calibration 60-Hz precision pulser was used to insert a line in the spectrum with an equivalent energy of about 18 keV. This pulser line was used as a secondary calibration line in the Ag spectra. Also the intensity of the pulser "line" was used to correct for electronic dead time at tandem energies. Above 15 MeV the cyclotron was used and, consequently, dead time corrections were obtained on the basis of the 5.90-keV peak produced by the ^{55}Fe source which was kept in a fixed position throughout the run. This was done because possible 60-Hz modulation of the cyclotron beam could make the 60-Hz-pulser dead time corrections unreliable.

III. RESULTS AND DISCUSSION

A. K and L X-Ray Yields, Cross Sections, and Ratios

The K and L x-ray yields $Y_{K,L}$ for Ag were calculated from the formula $Y_{K,L} = N_{\text{obs}} / A \epsilon_{\text{ctr}} Q t \Omega$, where $Y_{K,L}$ is the number of K or L x rays per sr per atom/cm². N_{obs} is the number of observed counts in the photo peak, the factor A is the correction for attenuation of the x-ray flux by self-absorption in the target, the Mylar window, the air path, and the beryllium window, ϵ_{ctr} is the efficiency of the counter, Q is the number of protons incident on the target, t is the target thickness in atoms/cm², and Ω is the solid angle subtended by the counter. The self-absorption correction was significant only for the L x rays. The following corrections were made for relative detection efficiencies: Ag $K\alpha = 0.86$, $K\beta = 0.71$, and $L = 0.098$, all $\pm 5\%$ except for the L , which was $\pm 10\%$, and for peak/total ratio (0.70 ± 0.02) of the Si(Li) detector. Assuming isotropy for the emitted K and L x rays, the absolute cross section for K -, L -shell x-ray production is then just

$$\sigma_{K,L \text{ x ray}} = 4\pi Y_{K,L} \quad (1)$$

and the cross sections for K -, L -shell ionization are obtained from Eq. (1) by correcting for Auger (and Coster-Krönig) nonradiative transitions using the fluorescence yield, ω_K or $\bar{\omega}_L$, as follows:

$$\sigma_{K,L} = 4\pi Y_{K,L} / \omega_{K,L} \quad (2)$$

The fluorescence yield for the Ag K shell was taken to be $\omega_K = 0.821 \pm 0.019$,²⁰ while the mean fluorescence yield used for the L shell was $\bar{\omega}_L = 0.047 \pm 0.002$.²¹ Recent theoretical calculations²² of the Auger and Coster-Krönig yields do not affect these results significantly.

The experimental K - and L -shell ionization cross

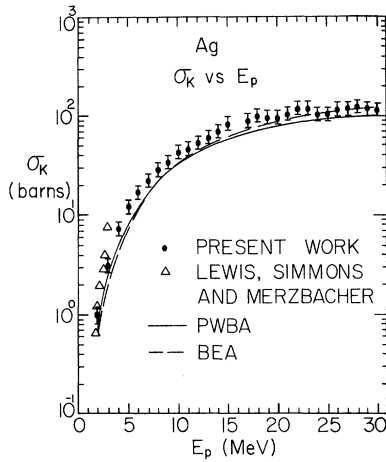


FIG. 2. σ_K for protons on Ag, ●, experimental results, present work; Δ , experimental results from Ref. 3; solid line, PWBA calculations from Ref. 7; dashed line, BEA calculations scaled from Mg from Ref. 2.

sections derived from K and L x-ray yields for proton bombardment of Ag which are given in Table I are shown in Figs. 2 and 3, respectively, along with the results for σ of Lewis, Simmons, and Merzbacher³ for proton energies from 1.70 to 2.88 MeV. Other measurements of σ_K for proton energies below 1 MeV are also available.^{23,24} Also shown in Figs. 2 and 3 are the PWBA and BEA predictions for σ_K and σ_L . These PWBA cross sections have been calculated using the following general formula:

$$\sigma_s = (8\pi z^2 a_0^2 / Z_s^4) (f_s / \eta_s), \quad (3)$$

where a_0 is the Bohr radius for hydrogen, z is the

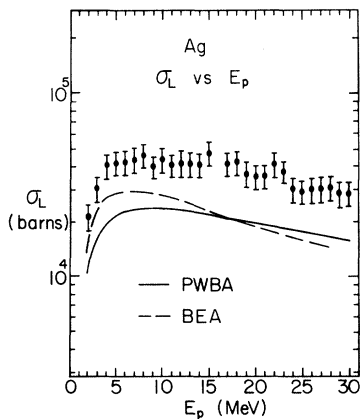


FIG. 3. σ_L for protons on Ag, ●, experimental results, present work; solid line, PWBA calculations from Ref. 7; dashed line, BEA calculations scaled from Mg from Ref. 2.

projectile charge, and Z_s is the screened target charge ($Z_K = Z - 0.3$, $Z_L = Z - 4.15$). The quantity η is defined as

$$\eta_s = (m/MZ_s^2)(E/\mathcal{R}_\infty), \quad (4)$$

where m and M are the electron and projectile mass and E is the projectile energy. The term f_s in Eq. (3) must be numerically evaluated for each choice of screening constant θ_s , where θ_s is defined as

$$\theta_s = I_s S^2 / (Z_s^2 \mathcal{R}_\infty). \quad (5)$$

I_s is the binding energy for the K or L shell ($s=1, 2$ for K, L shell and \mathcal{R}_∞ is the Rydberg constant).

For the L shell $f_s = f_{L1} + f_{L2} + f_{L3}$. The PWBA cross sections have been calculated⁷ using the following values for the screening constant θ : for the K shell $\theta_K = 0.86$; for the L subshell; $\theta_{L1} = 0.62$; $\theta_{L2} = 0.56$; $\theta_{L3} = 0.54$. The BEA cross sections for K -shell ionization were scaled from those given for Mg in Ref. 2, using the procedure described by Garcia. In this manner, σ_K for Ag can be scaled from the values for Mg:

TABLE I. Ag K and L x-ray and K - and L -shell ionization cross sections.

| E_p (MeV) | σ_K x ray ^a (b) | σ_K/ω_K ^b (b) | σ_L x ray ^c (kb) | σ_L/ω_L ^d (kb) |
|----------------|--------------------------------------|---|---------------------------------------|--|
| 2 | 0.81 | 1.0 | 0.97 | 21 |
| 3 | 2.6 | 3.2 | 1.4 | 31 |
| 4 | 6.1 | 7.4 | 1.9 | 40 |
| 5 | 10 | 12 | 2.0 | 42 |
| 6 | 14 | 17 | 2.0 | 44 |
| 7 | 19 | 23 | 2.0 | 44 |
| 8 | 24 | 29 | 2.2 | 46 |
| 9 | 29 | 35 | 1.9 | 40 |
| 10 | 36 | 44 | 2.0 | 44 |
| 11 | 39 | 48 | 1.9 | 41 |
| 12 | 44 | 54 | 2.0 | 42 |
| 13 | 50 | 61 | 1.9 | 41 |
| 14 | 57 | 69 | 1.9 | 41 |
| 15 | 59 | 84 | 2.2 | 48 |
| 17 | 74 | 90 | 1.9 | 41 |
| 18 | 82 | 100 | 2.0 | 42 |
| 19 | 79 | 96 | 1.7 | 37 |
| 20 | 79 | 96 | 1.7 | 35 |
| 21 | 86 | 104 | 1.7 | 36 |
| 22 | 98 | 119 | 1.9 | 41 |
| 23 | 98 | 119 | 1.8 | 38 |
| 24 | 84 | 102 | 1.4 | 30 |
| 25 | 85 | 104 | 1.4 | 29 |
| 26 | 95 | 116 | 1.4 | 30 |
| 27 | 96 | 117 | 1.4 | 30 |
| 28 | 95 | 115 | 1.4 | 29 |
| 30 | 92 | 112 | 1.3 | 28 |

^aAll cross sections are $\pm 15\%$.

^b $\omega_K = 0.821$, Ref. 20.

^cAll cross sections are $\pm 20\%$.

^d $\omega_L = 0.047$, Ref. 21.

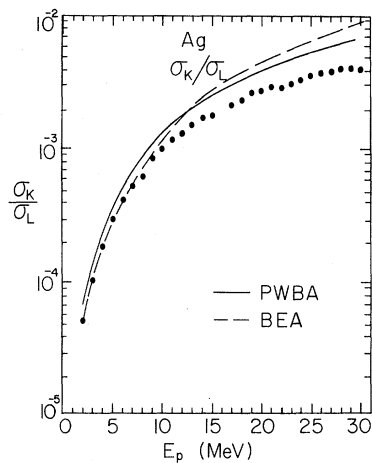


FIG. 4. σ_K/σ_L for protons on Ag. ●, experimental results, present work; solid line, PWBA calculations from Ref. 7; dashed line, BEA calculations scaled from Mg from Ref. 2.

$$\sigma_K(I_K(Ag), E^*) = \left(\frac{I_K(Mg)}{I_K(Ag)} \right)^2 \sigma(I_K(Mg), E),$$

where $E^* = [I_K(Ag)]/[I_K(Mg)]E$. This same procedure was employed for the L shell, using cross-section values for Mg above 4.85 MeV provided by Garcia. The agreement between experiment and either theoretical prediction is quite good for K -shell ionization.

The agreement for the case of L -shell ionization is not as good, however. Both the PWBA and BEA predictions fall below the experimental points, with the BEA curve coming more rapidly to a peak in σ_L and dropping more rapidly, while the PWBA curve falls approximately a factor of 2 too low over the whole proton-energy range. The PWBA curve more closely approaches the observed energy dependence in σ_L . The disagreement of predicted magnitudes of σ_L with the experimental values is quite possibly due to the value of $\bar{\omega}_L$ used to convert x-ray production cross sections to L -shell ionization cross sections. The quantity $\bar{\omega}_L$ is determined from orbital-electron-capture ratios and essentially defines a fixed average ionization state for each subshell of the L shell. Clearly, this same ionization state cannot be expected to pertain in the case of heavy-ion bombardment.

In Fig. 4 the experimental and PWBA and BEA theoretical absolute cross-section ratios σ_K/σ_L are shown versus proton energy. This experimental ratio cancels out target thickness, target-thickness variations, dead time corrections, current integration, etc., allowing a somewhat more stringent comparison to theoretical predictions. The agreement between experiment and PWBA theory over two orders of magnitude in this ratio

is good, considering the use of $\bar{\omega}_L$ to correct the x-ray yield. It is interesting to note that the PWBA calculation for σ_K/σ_L is larger than experiment by an approximately constant factor. The BEA prediction for σ_K/σ_L lies below the PWBA curve at lower proton energies, crossing it at about 13 MeV and steadily increasing over the PWBA curve until at 30 MeV it is 50% higher. This prediction is not in good agreement with the experimentally observed behavior of σ_K/σ_L .

B. $K\alpha/K\beta$ X-Ray Intensity Ratios

The Ag $K\alpha$ and $K\beta$ lines, which were well separated in this work (Fig. 1), maintain a constant ratio of intensities for proton energies from 2–30 MeV (see Fig. 5 and Table II). This constant ratio for $K\alpha/K\beta$ versus beam energy is not seen for ^{16}O beams on this same target; the $K\alpha/K\beta$ ratios for ^{16}O beams on a Ag target have been found to increase with increasing bombarding energy.¹⁴ Similar behavior is seen for the $K\alpha/K\beta$ ratio for other atoms subjected to ^{16}O beam bombardments.⁶ The average value for the $K\alpha/K\beta$ ratio for proton bombardment of Ag, corrected for relative detection efficiencies, is 4.68 ± 0.33 . The main source of error (7%) is in the relative detection-efficiency correction. This result is quite close to the $K\alpha/K\beta$ ratio measured for a thin ^{109}Cd source (4.83 ± 0.35). The $K\alpha/K\beta$ ratio measured from this ^{109}Cd is in good agreement with that $K\alpha/K\beta$ ratio for Ag (4.74 ± 0.09) reported by Hansen *et al.*²⁵ It agrees well with results of Mistry and Quarles²⁶ who excite these lines with 40–140 keV electrons and obtain 4.72 ± 0.09 . These results fall slightly below the theoretical results of Scofield, who used relativistic Hartree-Slater theory with a central potential and included retardation effects. He estimated that the calculated $K\alpha/K\beta$ ratios should be accurate to about 2% for Ag assuming only $E1$ decays, owing to

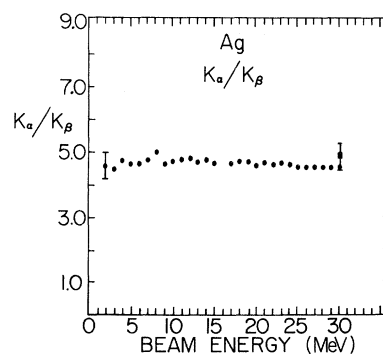


FIG. 5. $K\alpha/K\beta$ x-ray intensity ratios for Ag. ●, experimental results for protons on Ag, present work; ■, experimental results for 30-MeV $^{16}\text{O}^{5+}$ ions on Ag, present work.

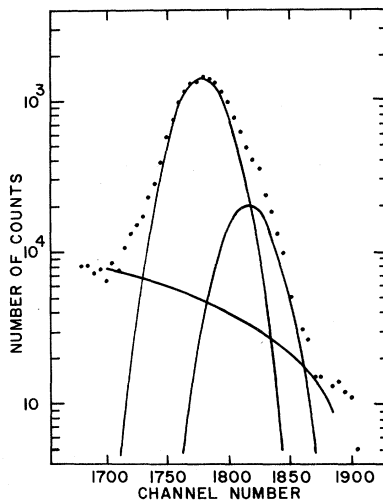


FIG. 6. Decomposition of a typical composite K peak into $K\beta_{1,3}$ and $K\beta_2$.

uncertainties in x-ray and binding energies. Thus the systematic result over all Z and all modes of excitation except heavy-ion bombardment that the $K\alpha/K\beta$ ratio lies 10–15% below theory is interesting, and would indicate that further theoretical refinements are in order.

C. $K\beta_{1,3}/K\beta_2$ X-Ray Intensity Ratios

The $K\beta$ line from Ag as seen with our Si(Li) detector has two major components (Fig. 6): $K\beta_{1,3}$, comprised of the $3p \rightarrow 1s E1$ transitions, and $K\beta_2$, comprised of the $4p \rightarrow 1s E1$ transitions. The $K\beta_{1,3}$ lines fall at about 24.9 keV, while the $K\beta_2$ line lies at about 25.5 keV. The $K\beta_4$ and $K\beta_5$ lines which correspond to the $3d \rightarrow 1s$ and $4d \rightarrow 1s E2$ transitions are expected to be much weaker. Scofield's calculations of the radiative widths for these lines indicate that they would constitute only about 0.5% of the intensity of the $K\beta$ composite peak. Since it was felt that the $K\beta_{1,3}/K\beta_2$ ratio was of interest, especially its energy dependence, an attempt was made to decompose the $K\beta$ peak into its two major components, using the Gauss-fit program. However, the poor resolution, combined with the rela-

tive weakness of the $K\beta_2$ component, did not produce reliable decomposition of $K\beta$. The widths of the two components were then constrained to be equal (although the $K\beta_{1,3}$ component is somewhat broader), and this permitted relatively reliable decomposition of $K\beta$, with separation between the two main components in quite good agreement with the expected 600-eV separation. The results of these double Gaussian fits to the $K\beta$ line are shown in Fig. 7 for proton energies from 3–30 MeV. The 2-MeV point was too weak for a reliable fit. The error bars shown, which hover between 7 and 10% over most of the region covered, were taken directly from the fitting program.

Fitting the $K\beta$ line produced by a ^{109}Cd source gave the result $K\beta_{1,3}/K\beta_2 = 4.97 \pm 0.3$, which can be compared with 6.00 ± 0.34 for this ratio obtained using a Kevex detector with 200-eV resolution at 6 keV, and fitting the data with a double Gaussian with no constraints. The latter measurement is expected to be most reliable, since the two components were well separated. Theory¹⁵ predicts 6.01 for this ratio.

Unfortunately, the Kevex detector was not available for the measurements with beam-induced x rays. However, the results for the detector with lower resolution still indicate that the $K\beta_{1,3}/K\beta_2$ ratio for proton-induced x rays is consistently higher than that observed for the ^{109}Cd source and seems to decrease slowly with increasing proton energy.

IV. SUMMARY

The experimental evidence obtained to date on K -shell ionization by proton bombardment indicates that for energies greater than ~ 500 times the binding energy of the K -shell electron, the semiclassical predictions of either the PWBA or BEA theory are in good agreement with experimental results both in the magnitude and projectile energy dependence of the cross section when reliable values of

TABLE II. $K\alpha/K\beta$ x-ray intensity ratios.

| Experiment | ^{47}Ag $K\alpha/K\beta$ | Reference |
|---|--------------------------------------|--------------|
| 2–30-MeV protons | 4.68 ± 0.33 | Present work |
| $^{109}\text{Cd}(\text{EC})^{109}\text{Ag}$ | 4.83 ± 0.35 | Present work |
| $^{109}\text{Cd}(\text{EC})^{109}\text{Ag}$ | 4.74 ± 0.09 | Ref. 25 |
| 40–140-keV electrons | 4.72 ± 0.09 | Ref. 26 |
| Theory | 5.09 ± 0.10 | Ref. 15 |

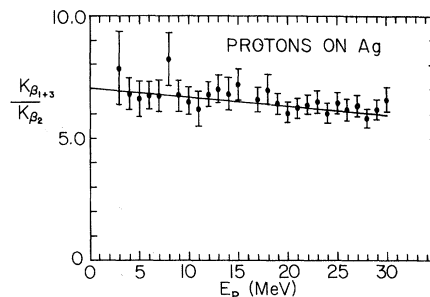


FIG. 7. $K\beta_{1,3}/K\beta_2$ x-ray intensity ratios for Ag. The straight line is a least-squares fit to the data. Its slope is -0.0322 ± 0.0133 per MeV and its intercept is 7.072 ± 0.278 .

ω_K are used. At lower energies and for $Z \lesssim 30$, the BEA theoretical predictions as well as those of Bang and Hansteen,⁸ which make some attempt to correct for the effect of nuclear repulsion of the projectile, are closer to the experimental results than the PWBA predictions. However, the low-energy discrepancy between PWBA and BEA predictions grows less as Z increases. For Ag (see Fig. 3) the BEA and PWBA predictions almost overlap in the region 2–13 MeV, diverging slightly above this. Relativistic corrections^{27,28} to the atomic wave functions are not expected to produce any significant changes in the PWBA predictions for σ_K and σ_L for Ag.

There was no evidence for energy shifts in the $K\alpha$ and $K\beta$ lines in Ag as proton energy was varied, nor was any significant energy difference observed between the proton-induced lines and those produced by a ^{109}Cd source. No significant variation in the $K\alpha/K\beta$ ratio with proton energy was observed, either, which agrees with the experimentally observed fact that energy shifts in the $K\alpha$ and $K\beta$ lines are accompanied by variations in the $K\alpha/K\beta$ ratio.^{6,14} The $K\alpha/K\beta$ ratios determined experimentally for Ag (see Table II) consistently fall below Scofield's prediction. The $K\beta_{1,3}/K\beta_2$ ratio for the ^{109}Cd source x rays agrees with that predicted by Scofield, for the high-resolution mea-

surements. The $K\beta_{1,3}/K\beta_2$ ratios from the proton-induced x rays all seem to be consistently above the ratio measured for the ^{109}Cd source and seem to decrease slightly with increasing proton energy.

The semiclassical theories are seen to fail for $Z \geq 2$ projectiles, and the disagreement seems to increase with the Z of the projectile. The Coulomb deflection and binding-energy corrections to PWBA predictions do seem to improve agreement²⁹ with experimentally measured K -shell ionization cross sections. However, the effect on transition rates for radiative versus nonradiative processes of an atom being left in a state of multiple inner-shell ionization due to heavy-ion bombardment requires further work, as does the theory which would predict cross sections for multiple inner-shell ionization.

ACKNOWLEDGMENTS

We are grateful to Dr. E. Merzbacher for encouragement and many helpful discussions relating to this work. We wish to thank Dr. G. Basbas and Dr. J. D. Garcia for communicating results to us before publication. We wish to acknowledge work by James Howard and David Peterson, who helped in recording the data and worked on the efficiency calibration of the detector.

[†]Work performed under the auspices of the U. S. Atomic Energy Commission.

*Present address: Rutgers University, New Brunswick, N. J. 08903.

¹E. Merzbacher and H. W. Lewis, *Encyclopedia of Physics*, edited by S. Flügge (Springer, Berlin, 1958), Vol. 34, p. 166. This work and Refs. 2 and 3 provide a reasonably complete summary of presently available experimental work on K -shell ionization by protons.

²J. D. Garcia, *Phys. Rev. A* **1**, 280 (1970); **1**, 1402 (1970); and private communication.

³H. W. Lewis, E. B. Simmons, and E. Merzbacher, *Phys. Rev.* **91**, 943 (1953); E. M. Bernstein, H. W. Lewis, and W. R. Wisseman (unpublished).

⁴J. M. Khan, D. L. Potter, and R. D. Worley, *Phys. Rev.* **139**, A1735 (1965); **145**, 23 (1966); R. R. Hart, F. W. Reuter, III, H. P. Smith, Jr., and J. M. Khan, *ibid.* **179**, 4 (1969).

⁵G. A. Bissinger, J. M. Joyce, E. J. Ludwig, W. S. McEver, and S. M. Shafroth, *Phys. Rev. A* **1**, 841 (1970).

⁶P. Richard, T. I. Bonner, T. Furuta, I. L. Morgan, and J. R. Rhodes, *Phys. Rev. A* **1**, 1044 (1970).

⁷G. S. Khandelwal, B. H. Choi, and E. Merzbacher, *At. Data* **1**, 103 (1969).

⁸J. Bang and J. M. Hansteen, *Kgl. Danske Videnskab. Selskab, Mat.-Fys. Medd.* **32**, No. 13 (1959).

⁹G. Basbas, W. Brandt, and R. Laubert, *Phys. Letters* **34A**, 277 (1971).

¹⁰C. W. Lewis, J. B. Natowitz, and R. L. Watson, *Phys. Rev. Letters* **26**, 481 (1971).

¹¹W. Brandt, R. Laubert, and I. Sellin, *Phys. Rev.* **151**, 56 (1966).

¹²R. C. Der, T. M. Kavanagh, J. M. Khan, B. P. Curry, and R. J. Fortner, *Phys. Rev. Letters* **21**, 1731 (1968).

¹³D. Burch and P. Richard, *Phys. Rev. Letters* **25**, 983 (1970).

¹⁴G. A. Bissinger, P. H. Nettles, S. M. Shafroth, and A. W. Waltner, *Bull. Am. Phys. Soc.* **16**, 545 (1971).

¹⁵James H. Scofield, *Phys. Rev.* **179**, 9 (1969).

¹⁶P. Richard, I. L. Morgan, T. Furuta, and D. Burch, *Phys. Rev. Letters* **23**, 1009 (1969).

¹⁷G. A. Bissinger, S. M. Shafroth, and A. W. Waltner, *Bull. Am. Phys. Soc.* **16**, 125 (1971).

¹⁸H. W. Newson, F. D. Purser, N. R. Roberson, E. G. Bilpuch, R. L. Walter, and E. J. Ludwig, *Bull. Am. Phys. Soc.* **14**, 533 (1969).

¹⁹L. B. Magnusson, *Phys. Rev.* **107**, 161 (1957).

²⁰C. E. Roos, *Phys. Rev.* **105**, 931 (1957).

²¹R. W. Fink, R. G. Japson, Hans Mark, and C. D. Swift, *Rev. Mod. Phys.* **38**, 513 (1966).

²²V. O. Koshoun, M. H. Chen, and B. Craseman, *Phys. Rev. A* **3**, 533 (1971); and private communication.

²³S. Messelt, *Nucl. Phys.* **5**, 435 (1958).

²⁴B. Singh, *Phys. Rev.* **107**, 711 (1957).

²⁵J. S. Hansen, H. U. Freund, and R. W. Fink, *Nucl. Phys.* **A142**, 604 (1970).

²⁶W. D. Mistry and C. A. Quarles, *Nucl. Phys.* **A164**, 219 (1971).

²⁷D. Jamnik and C. Zupancic, *Kgl. Danske Videnskab. Selskab, Mat.-Fys. Medd.* **31**, No. 2 (1957).

²⁸B. H. Choi, *Phys. Rev. A* **4**, 1971.

²⁹D. Burch and P. Richard (private communication).